

# Computationally Efficient Design Optimization of Compact Microwave and Antenna Structures

Slawomir Koziel, Piotr Kurgan and Adrian Bekasiewicz

**Abstract** Miniaturization is one of the important concerns of contemporary wireless communication systems, especially regarding their passive microwave components, such as filters, couplers, power dividers, etc., as well as antennas. It is also very challenging, because adequate performance evaluation of such components requires full-wave electromagnetic (EM) simulation, which is computationally expensive. Although high-fidelity EM analysis is not a problem for design verification, it becomes a serious bottleneck when it comes to automated design optimization. Conventional optimization algorithms (both gradient-based and derivative-free ones such as genetic algorithms) normally require large number of simulations of the structure under design, which may be prohibitive. Considerable design speedup can be achieved by means of surrogate-based optimization (SBO) where a direct handling of the expensive high-fidelity model is replaced by iterative construction and re-optimization of its faster representation, a surrogate model. In this chapter, we review some of the recent advances and applications of SBO techniques for the design of compact microwave and antenna structures. Most of these methods are tailored for a design problem at hand, and attempt to utilize its particular aspects such as a possibility of decomposing the structure. Each of the methods exploits an underlying low-fidelity model, which might be an equivalent circuit, coarse-discretization EM

---

S. Koziel (✉) · A. Bekasiewicz  
Engineering Optimization & Modeling Center,  
School of Science and Engineering, Reykjavik University,  
Menntavegur 1, 101 Reykjavik, Iceland  
e-mail: koziel@ru.is

A. Bekasiewicz  
e-mail: bekasiewicz@ru.is

P. Kurgan  
Faculty of Electronics, Telecommunications and Informatics,  
Gdansk University of Technology, 11/12 Narutowicza Street,  
80-233 Gdansk, Poland  
e-mail: piotr.kurgan@eti.pg.gda.pl

simulation data, and approximation model, or a combination of the above. The common feature of the presented techniques is that a final design can be obtained at the cost of a few evaluations of the high-fidelity EM-simulated model of the optimized structure.

**Keywords** Microwave engineering · Simulation-driven design · Surrogate modeling · Surrogate-based optimization · Compact structures · Expensive optimization problems

## 1 Introduction

Small size is one of the most important requirements imposed upon modern wireless communication system blocks, with particular emphasis on microwave passive components [1, 2], including, among others, filters [3–6], couplers [7–10], power dividers [11–14], as well as antennas [15–18]. Satisfying strict electrical performance specifications and achieving compact size are normally conflicting objectives [19–22]. These difficulties can be alleviated to some extent, e.g., through replacing conventional transmission lines by their more compact counterparts such as slow-wave resonant structures (SWRSs) [23–26], or, in case of antennas, by introducing certain topological modifications (e.g., stubs and slits in ground planes of ultra-wideband antennas [27–29]). At the same time, the use of traditional design techniques based on equivalent circuit models does not lead to reliable results due to considerable electromagnetic (EM) couplings between circuit components within highly compressed layouts that cannot be accurately accounted for at the network level. Reliable evaluation of the structure performance is only possible by means of CPU-intensive and time-consuming full-wave EM simulations.

Unfortunately, EM analysis may be computationally expensive, even when using vast computing resources: simulation time with fine discretization of the structure may be from 15–30 min for simple passive microwave circuits and small antennas [24, 25, 28], to a few hours for more complex structures (e.g., miniaturized Butler matrix [30]). This creates a serious bottleneck for automated, EM-simulation-driven design optimization of compact circuits: conventional optimization methods (such as gradient-based routines [31, 32], or derivative-free methods, e.g., pattern search [33] or population-based metaheuristics [34–36]) normally require large number of objective function evaluations, each of which is already expensive. The use of adjoint sensitivities [37, 38] allows—to some extent—for reducing design optimization cost, however, this technology is not yet widespread in microwave and antenna community, especially in terms of its availability through commercial simulation software packages (with some exceptions, e.g., [39, 40]). Heuristic simulation-based design approaches, typically exploiting parameter sweeps guided by engineering experience, tend not to work for compact structures because the latter are characterized by many designable parameters as well as optimum parameter setups are often counter-intuitive.

Reducing the computational efforts of microwave/antenna design processes, especially in the context of compact structures, is of fundamental importance for design automation and lowering the overall design cost (both in terms of computational resources and time), which, consequently, has implications for economy, environmental protection, as well as the quality of life. Thus, it is important from the point of view of computational sustainability.

Probably the most promising approach in terms of computationally efficient design is surrogate-based optimization (SBO) [41, 42]. In SBO, direct optimization of the expensive high-fidelity simulation model is replaced by iterative updating and re-optimization of its computationally cheap representation, the surrogate. As a result of shifting the optimization burden into the surrogate, the overall design cost can be greatly reduced. The high-fidelity model is referenced rarely, to verify the prediction produced by the surrogate and to improve the latter. Various SBO methods differ mostly in the way the surrogate is created. There is a large class of function approximation modeling techniques, where the surrogate is created by approximating sampled high-fidelity model data. The most popular methods in this group include polynomial approximation [43], radial basis function interpolation [44], kriging [43, 45], support vector regression [46], and artificial neural networks [47, 48]. Approximation models are very fast but a large number of training samples are necessary to ensure reasonable accuracy. Also, majority of approximation techniques suffer from the so-called *curse of dimensionality* (i.e., an exponential growth of required number of training samples with the dimensionality of the design space, [36]). Depending on the model purpose, this initial computational overhead may (e.g., multiple-use library models) or may not (e.g., one-time optimization) be justified.

An alternative approach to creating surrogate models is by correcting an underlying low-fidelity (or coarse) model. The latter is a simplified representation of the structure (system) under design. It can be obtained, among others, by using a different level of physical description of the system (e.g., equivalent circuit versus full-wave electromagnetic simulation in case of microwave or antenna structures), or through the same type of simulation as utilized by the high-fidelity model but with coarser structure discretization, relaxed convergence criteria, etc. As opposed to approximation models, low-fidelity models are stand-alone models embedding some knowledge about the system of interest [49]. Therefore, physics-based surrogates normally exhibit much better generalization capability [25, 50]. Consequently, considerably smaller amount of training data is required to ensure sufficient accuracy of the model. Some more or less known SBO techniques exploiting physics-based surrogates include approximation model management optimization (AMMO) framework [51], space mapping (SM) [52, 53], manifold mapping [54, 55], and simulation-based tuning [56, 57].

In this chapter, we review some of the recent advances and applications of SBO techniques for the design of compact microwave and antenna structures. While some of the discussed methods are rather standard (e.g., space mapping with additive response correction utilized for ultra-wideband antenna optimization), others are more tailored for a design problem at hand, and attempt to utilize its particular aspects such as a possibility of decomposing the structure of interest. Each of the

methods exploits an underlying low-fidelity model, which might be an equivalent circuit, coarse-discretization EM simulation data, and approximation model, or a combination of the above. The common feature of the presented techniques is that a final design can be obtained at the cost of a few evaluations of the high-fidelity EM-simulated model of the optimized structure.

The chapter is organized as follows. In Sect. 2, we briefly highlight the design challenges for miniaturized microwave and antenna components and emphasize the necessity of using—in the design process—high-fidelity electromagnetic simulations, as well as the need for computationally efficient techniques aimed at reducing computational cost of the process. In Sect. 3, we formulate the microwave design optimization problem, discuss electromagnetic simulation models, and introduce the concept of surrogate-based optimization (SBO). Sections 4, 5, and 6 showcase three selected case studies concerning the design of compact branch-line couplers, compact radio frequency (RF) components, and miniaturized ultra-wideband antennas. While each of these sections describes optimization techniques exploiting the SBO paradigm, methodological details are developed to handle problem-specific design challenges. We also present numerical results, as well as comparisons with benchmark techniques. An emphasis is on computational savings that can be obtained by using a suitable combination of surrogate-modeling and variable-fidelity simulations (both at the equivalent circuit and full-wave electromagnetic level). Section 7 concludes the chapter.

## 2 Challenges of Compact Microwave Structure Design

Reliable development of compact microwave circuits is the subject of intense research in the field of microwave and antenna engineering [58–60]. Miniaturized microwave and antenna components can be extensively utilized as fundamental building blocks of modern wireless communication systems that are continuously challenged with ever more severe specifications: higher performance, smaller size, lighter weight, and lower cost. The fundamental problem of small-size microwave and antenna structure development process is to find a design that satisfies a given specification, within a tight computational budget, and providing highly accurate results. However, the accomplishment of this goal poses extremely difficult obstacles from the methodological point of view.

A typical microwave circuit with a compact footprint is constructed from non-uniform transmission lines that mimic the electrical performance of their conventional counterparts in a limited frequency range, but at the same time offer reduced physical dimensions, which can lead to a smaller size of the circuit [59–81]. Most commonly, T-networks [59, 61–67] or  $\pi$ -networks [59, 65, 68–73] are chosen for the purpose of non-uniform transmission line realization. Such simple circuits can be analyzed with ease by means of transmission line theory, which leads to relatively accurate results, assuming the lack of cross-coupling effects and a negligible influence of other high-frequency phenomena (e.g., anisotropy of the substrate, current

crowding, etc.) on the performance of a microwave component. This supposition, however, is valid only for conventional circuits [80]. It should be underlined that—in case of highly compact microwave and antenna structures with complex and closely fit building blocks within a layout—the use of simplified theory-based models is limited to providing initial design solutions that indispensably require further EM fine-tuning [7, 61–66, 71, 72, 76, 77, 79]. In order to produce accurate results, it is preferable to apply a high-fidelity EM analysis from the early stages of the design process of miniaturized microwave components [81, 82]. Similarly, the use of theoretical models in contemporary antenna engineering is an outdated practice that cannot provide information on complex EM phenomena taking place in the antenna structure under consideration. This is particularly true in case of unconventional antennas with complex and compact footprints. For the above-mentioned reasons, EM-simulation-driven design is nowadays a necessity in computer-aided design of microwave and antenna devices [79, 83].

On the other hand, exploitation of EM simulation tools, either throughout the entire design process or in the design closure eventually leads to high demands on enormous computational resources. The main issue here lies in the numerical cost associated with the high-fidelity EM analysis of the entire compact component. In case of conventional EM-driven design approaches, based either on laborious parameter sweeps [9] or direct single-objective optimization [79, 83] (gradient-based or derivative-free), this becomes impractical or even prohibitive when handling computational demands of miniaturized passives. The problem becomes even more profound when the design process is realized in more general setting, i.e., when it entails adjustment of designable parameters of the structure to satisfy multiple, often conflicting objectives such as size, bandwidth, phase response, etc. [20], in case of microwave components, and size, return loss, gain, etc., in case of antenna structures [84]. This, however, illustrates a multi-objective optimization problem, which is far more challenging than the single-objective one. For typical examples of compact microwave or antenna structures—that are characterized by a number of designable parameters—the design process aimed at finding a set of trade-offs between conflicting objectives cannot be accomplished using traditional multi-objective algorithms such as population-based metaheuristics [34, 35], because these require a massive number of objective function evaluations (thousands or tens of thousands), which in case of high-fidelity EM models is prohibitive within a reasonable time-frame [36, 84].

### **3 Optimization Problem Formulation. Electromagnetic Models. Surrogate-Based Optimization**

In this section, we formulate the microwave/antenna optimization problem, discuss various types of models utilized in microwave engineering, as well as recall the basics of surrogate-based optimization (SBO) [32]. The specific SBO techniques developed

and utilized for expedited design of compact microwave and antenna structures are discussed in Sects. 4 through 6.

### 3.1 Microwave Optimization Problem

The microwave design optimization problem can be formulated as

$$\mathbf{x}^* = \arg \min_{\mathbf{x}} U(\mathbf{R}_f(\mathbf{x})) \quad (1)$$

where  $\mathbf{R}_f(\mathbf{x}) \in R^m$ , denotes the response vector of a high-fidelity (or fine) model of the device or system of interest. In microwave engineering, the response vector may contain, for example, the values of so-called scattering parameters [1] evaluated over certain frequency band. The objective function  $U : R^m \rightarrow R$  is formulated so that a better design corresponds to a smaller value of  $U$ . Often, the design specifications are formulated in a minimax sense [85], e.g., in the form of minimum/maximum levels of performance parameters for certain frequency bands.

In many situations, it is necessary to consider several design objectives at a time (e.g., gain, bandwidth, layout area). The objectives usually conflict with each other and the design process aims at finding a satisfactory trade-off between them. However, genuine multi-objective optimization exceeds the scope of this chapter. Thus, although multiple objectives are actually present in all the design cases discussed in Sects. 4–6, they are handled by a priori preference articulation, i.e., selecting the primary objective and controlling the others either through appropriately defined constraints or penalty functions [13].

### 3.2 Simulation Models in Microwave Engineering

The most important simulation models utilized in microwave/antenna engineering include equivalent circuit (or network) models and electromagnetic (EM) simulation ones.

For decades, circuit models have been important tools microwave structure design. They provide a simplified structure representation by means of analytical equations that origin from the transmission line theory. The behavior of a structure is described using its complex impedance, capacitance and/or inductance [1, 86]. Construction of a circuit model representation of a structure is based on interconnection of basic building blocks (i.e., transmission lines, coupled lines, bends, tees, etc.) in such a way that the behavior of a model mimics the behavior of a real structure [87, 88], i.e., coupled lines represents the coupling within the circuit and tee represents the interconnection between transmission lines within a circuit, etc. Such a representation is very useful for variety of structures characterized by modular construction

(e.g. filters, couplers, matching transformers, etc.). Unfortunately, limited diversity of building blocks prohibits the design of unusual geometries. Moreover, circuit models are inaccurate that forces the utilization of electromagnetic simulations for final tuning of the structure. Another problem is that they lack of capability to estimate radiation field, which turns them useless for the design of antenna structures.

Antenna structures can be modeled using quasi-static representation [89]. Utilization of such models allows for i.e., estimation of antenna operating frequency, radiation pattern, and/or impedance matching. Empirical models are particularly useful if antenna design requires tremendous number of model evaluations (e.g., in multi-objective optimization [21, 84]). Despite fast evaluation, quasi-static representation suffers from considerable inaccuracy. Moreover, it is available only for some conventional designs, which turns empirical antenna representation not very popular nowadays.

The most generic and accurate way of representing microwave/antenna structures is full-wave electromagnetic simulation. The electromagnetic solvers utilize advanced meshing techniques aimed at discretization of the design into a set of sub-problems, which are evaluated by solving Maxwell’s equations [89, 90]. Despite its accuracy, such a representation suffers from considerable computational cost. Reduction of the simulation time can be obtained by introducing certain simplifications into the EM model, e.g., sparse mesh, modeling of metallization as infinitely thin sheet, neglecting losses of dielectric substrate, or utilization of perfect electric conductor instead of finite-conductivity metals. Usually the simplified model is 10 up to 50 times faster than the high-fidelity one. Coarse-mesh EM models are useful auxiliary tools utilized by many surrogate-based optimization methods [15, 91].

A conceptual illustration of a high- and low-fidelity EM model as well as a circuit model of an exemplary structure is provided in Fig. 1.

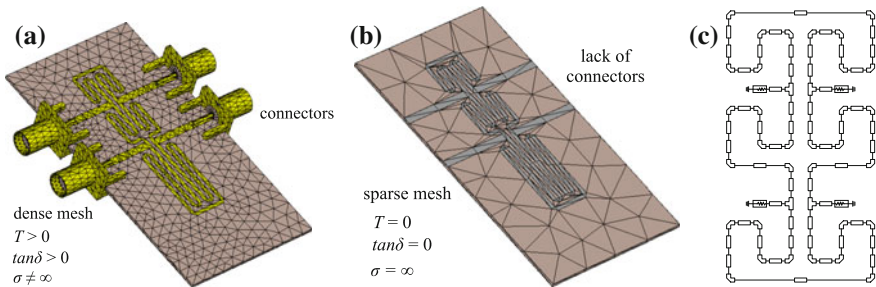


**Fig. 1** Various representations of the same rat-race coupler structure. **a** High-fidelity EM model representation; **b** simplified low-fidelity EM model (simplifications include: lack of connectors, coarse mesh, neglected metallization thickness and dielectric losses, as well as perfect conductivity of metallization); **c** circuit representation of the coupler—the fastest, yet the most inaccurate

### 3.3 Surrogate-Based Optimization

Our major concern is to reduce the cost of solving the optimization problem (1). As mentioned before, in many cases, direct handling of the high-fidelity model  $\mathbf{R}_f$  is not even possible either due to the high individual cost of evaluating  $\mathbf{R}_f$  or very large number of model evaluations when solving (1). Therefore, we are interested in surrogate-based optimization (SBO) [32] methods, where the sequence  $\mathbf{x}^{(i)}$ ,  $i = 0, 1, \dots$ , of approximate solutions to (1) is found by means of an iterative procedure [92]

$$\mathbf{x}^{(i+1)} = \arg \min_{\mathbf{x}} U(\mathbf{R}_s^{(i)}(\mathbf{x})) \quad (2)$$

Here,  $\mathbf{x}^{(i+1)}$  is the optimal design of the surrogate model  $\mathbf{R}_s^{(i)}$ ,  $i = 0, 1, \dots$ .  $\mathbf{R}_s^{(i)}$  is assumed to be a computationally cheap and sufficiently reliable representation of the high-fidelity model  $\mathbf{R}_f$ , particularly in the vicinity of the current design  $\mathbf{x}^{(i)}$ . Under these assumptions, the algorithm (2) is likely to produce a sequence of designs that quickly approach  $\mathbf{x}^*$ .

Because  $\mathbf{R}_f$  is evaluated rarely (usually once per iteration), the surrogate model is supposedly fast, and the number of iterations for a well-performing algorithm is substantially smaller than for most conventional optimization methods, the process (2) may lead to substantial reduction of the computational cost of solving (1). Moreover, if the surrogate model satisfies zero- and first-order consistency conditions with the high-fidelity model [51], i.e.,  $\mathbf{R}_s^{(i)}(\mathbf{x}^{(i)}) = \mathbf{R}_f(\mathbf{x}^{(i)})$  and  $\mathbf{J}_{R_s}^{(i)}(\mathbf{x}^{(i)}) = \mathbf{J}_{R_f}(\mathbf{x}^{(i)})$  with  $\mathbf{J}$  being a Jacobian of the respective model (verification of the latter requires  $\mathbf{R}_f$  sensitivity data), and the algorithm (2) is embedded in the trust region framework [93], then it is provably convergent to a local optimum of original problem (1). Convergence can also be guaranteed if the algorithm (2) is enhanced by properly selected local search methods [31].

Various SBO techniques mostly differ by the way of constructing the surrogate model. The specific techniques utilized to handle the design cases presented in this chapter are elaborated on in Sects. 4–6. Interested reader is referred to the literature (e.g., [19, 22, 85]) to find out more about other possible options.

## 4 Case Study I: Expedited Design of Compact Branch-Line Couplers

In this section, we present a design methodology based on [94], dedicated to efficient solving of complex and numerically demanding design problems of popular microwave components, i.e., branch-line couplers with compact footprints. This technique enables a cost-efficient and accelerated design optimization of the microwave component of interest together with high accuracy of the results. The desired performance of the circuit under design as well as its miniaturized layout are achieved by adjusting designable parameters of the non-uniform building blocks of the structure.



The proposed method can be divided into two separate stages: (i) concurrent EM optimization of non-uniform constitutive elements of the branch-line coupler (so-called composite cells), where cross-coupling effects between the adjacent cells are absent, and (ii) fine-tuning of the entire branch-line coupler exploiting space-mapping-corrected surrogate model, constituted by cascaded local response surface approximation models of the separate cells. The first stage is realized at a low computational cost (just a few evaluations of the entire branch-line coupler), because the mutual EM coupling between the cells is not taken into account. The second stage, in turn, accounts for any cross-coupling phenomena and other interactions between building blocks of the structure under design. We showcase the efficiency of the proposed technique by a numerical case and its experimental validation.

#### 4.1 Design Problem and Coupler Structure

Microstrip branch-line couplers (BLCs) are vital components widely used in many practical microwave and radio frequency circuits, such as balanced mixers [95], Butler matrixes [42], and others. An ideal BLC offers perfect transmission characteristics at a the operating frequency: an equal power splitting between the output ports with  $90^\circ$  phase shift, perfect matching with system impedance  $Z_0$ , and perfect isolation. In the vicinity of the operating frequency, usually within the 10% bandwidth, the performance of the circuit is still acceptable, however not ideal. A conventional BLC is composed of four quarter-wavelength uniform transmission lines, two of which are defined by  $Z_0$  characteristic impedance, while the rest are determined by  $0.707 \cdot Z_0$  characteristic impedance. In this case study, the task is to design a 3-dB BLC for operating frequency  $f_0 = 1$  GHz using Taconic RF-35 ( $\epsilon_r = 3.5$ ,  $h = 0.508$  mm,  $\tan\delta = 0.0018$ ) as a dielectric substrate. The intended bandwidth is 0.96–1.04 GHz with return loss and isolation  $|S_{11}|$ ,  $|S_{41}| \leq -20$  dB. For comparison purposes, a conventional BLC has been designed on the basis of [82]. Its exterior dimensions are: 45.6 mm  $\times$  48.1 mm. We use BLC parameterization shown in Fig. 2. It can be observed that the complementary building blocks almost completely fill the interior of the BLC. Dimensions of horizontal and vertical cell (denoted Cell<sub>1</sub> and Cell<sub>2</sub>, respectively) are given by vectors  $\mathbf{x}_1$  and  $\mathbf{x}_2$ . All parameters of Cell<sub>1</sub>,  $x_1, x_2, \dots, x_7$ , are independent, whereas Cell<sub>2</sub> is described by both independent,  $x_8, x_9, \dots, x_{12}$ , and dependent,  $y_1, y_2, y_3$ , parameters. The latter depend on specific parameters of Cell<sub>1</sub> and the predefined distance  $d$  between the cells. Parameterization of Cell<sub>1</sub> and Cell<sub>2</sub> is given by:  $f_1(\mathbf{x}) = f_1([x_1 x_2 \dots x_{12}]^T) = [x_1 x_2 \dots x_7]^T$  and  $f_2(\mathbf{x}) = f_2([x_1 x_2 \dots x_{12}]^T) = [x_8 x_9 \dots x_{12} y_1 y_2 y_3]^T$ , where  $y_1 = 0.5 \cdot (x_7 + d/2 - x_8 - 2 \cdot x_{10} - 2.5 \cdot x_{12})$ ,  $y_2 = x_1 + x_3 + x_4 + x_6 - d - x_{12}$  and  $y_3 = x_8 + x_{12} - d$ . Geometrical dependence between the non-uniform building blocks enables the preservation of consistency of the dimensions and a high miniaturization of the entire structure. In this example,  $d = 0.2$  mm.

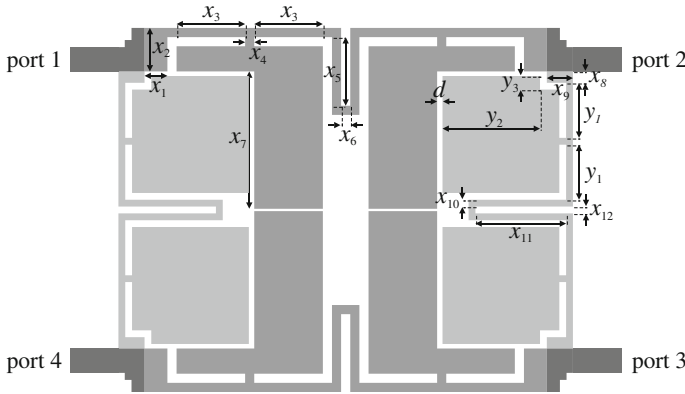


**Fig. 2** Parameterized BLC composed of Cell<sub>1</sub> (dark gray color, port impedance  $Z_0 = 35.35 \Omega$ ) and Cell<sub>2</sub> (light gray color, port impedance  $Z_0 = 50 \Omega$ )

## 4.2 Design Methodology

In this section, we present a specific surrogate-based optimization scheme dedicated for solving computationally complex design problems of compact branch-line couplers. In particular, we provide a general description of the proposed approach, together with a mathematical formulation of its subsequent steps, i.e., concurrent cell optimization, response surface approximation model construction, and surrogate-based design refinement.

### 4.2.1 General Design Scheme

An overview of the proposed design method is shown in Fig. 3a. The numerical efficiency of this technique stems from concurrent optimization detached non-uniform building blocks of a compact BLC, and subsequent surrogate-based fine-tuning of the entire component. The first stage is aimed at arriving at the optimized design of composite cells treated separately. It is noteworthy that the non-uniform building blocks of the compact coupler are geometrically dependent (to ensure the design consistency and size reduction of the BLC), but electromagnetically isolated (to lower the evaluation cost of their high-fidelity EM model). This has proven to be exceptionally beneficial from the numerical standpoint as it enabled the embedment—within a single optimization procedure—of two high-fidelity, yet reasonably cheap EM models representing BLC building blocks of interest instead of one CPU-intensive EM model of the entire BLC under development. The use of ultimately accurate simulation tool available for an engineer ensures us that the solution obtained in this manner lies in the neighborhood of the BLC optimized design.

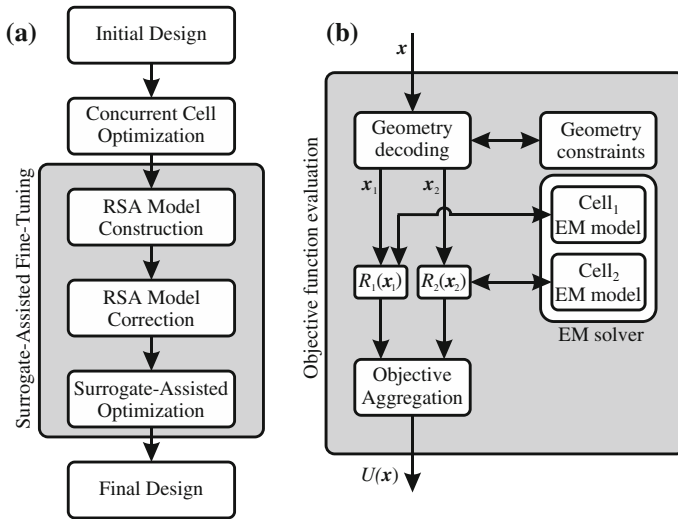


**Fig. 3** **a** Proposed design procedure of highly miniaturized BLCs; **b** Objective function evaluation for concurrent cell optimization

The following fine-tuning of the BLC is accomplished as a surrogate-based optimization process with the underlying low-fidelity model being a cascade of local response surface approximations (RSAs) of the optimized non-uniform building blocks of the BLC. Formally, this is an iterative process, however, as given by the case study (cf. Sect. 4.3), one iteration is completely sufficient.

The main benefit of the proposed method lies in the low computational cost required to obtain the optimized design, which is realized within a single and fully automated process. The most expensive model in the design problem under consideration—namely, high-fidelity EM model of the entire compact BLC—is evaluated only twice, i.e., at the initial design produced by the first stage, and for the verification of the final design.

### 4.2.2 Concurrent Cell Optimization

The simulation-driven design methodology discussed in this section offers a fully automated development of compact BLCs. However, it requires a manual setup of non-uniform building blocks of a miniaturized BLC. Wide collections of such composite cells can be found in the literature, e.g., in [82]. A typical BLC is composed of quarter-wavelength uniform transmission lines of  $Z_0$  and  $0.707 \cdot Z_0$  characteristic impedances to achieve an equal power split between the output ports, where  $Z_0$  is the system impedance [80].

Thus, in order to construct a small-size BLC, two complementary constitutive cells are needed. These are separated by a predefined distance  $d$  and intended to fill the interior of the BLC in a highly efficient manner. Geometry parameters of the cells are encoded in a parameter vector  $\mathbf{x}$ . Some designable parameters are independent; others are dependent to ensure geometrical fit of the cells. Formally, we describe this relation as  $\mathbf{x}_1 = f_1(\mathbf{x})$  and  $\mathbf{x}_2 = f_2(\mathbf{x})$ . In practice,  $f_1$  is a projection (i.e.,  $\mathbf{x}_1$  is composed of selected elements of the vector  $\mathbf{x}$ ), whereas  $f_2$  determines clearly specified geometry constraints to make both composite cells fit into a compact coupler layout. Specific realizations of these functions are shown in Sect. 4.1.

During the concurrent cell optimization stage of the entire design process, we exploit two separate high-fidelity EM models to take into consideration all internal electromagnetic effects present inside of a non-uniform cell, but neglecting any cross-coupling phenomena between adjacent cells. Such a formulation of the design task allows for performing a CPU-cheap concurrent optimization of both composite cells. The aggregated objective function  $U(\mathbf{x})$  for the cells is evaluated using given design specifications and cell response vectors  $R_i(\mathbf{x}_i)$ ,  $i = 1, 2$  (cf. Fig. 3b).

Design specifications pertaining to the cells under concurrent optimization are imposed by the transmission line theory [80]. We aim at obtaining a required phase shift  $\phi_c$ ,  $\arg(S_{21})$  at the operating frequency  $f_0$  as well as to minimize the return loss  $|S_{11}|$  at  $f_0$  and around it. The task is formulated as follows:

$$\mathbf{x}_c^* = \arg \min_{\mathbf{x}} U(\mathbf{x}) \quad (3)$$

where

$$U(\mathbf{x}) = \max_{f_0-df \leq f \leq f_0+df} \{|S_{11.1}(\mathbf{x}_1; f)|, |S_{11.2}(\mathbf{x}_2; f)|\} + \beta \sum_{i=1}^2 [\arg(S_{21.i}(\mathbf{x}_i; f_0)) - \phi_c]^2 \quad (4)$$

Here,  $\mathbf{x}$  is a vector of all designable parameters,  $\mathbf{x}_i$ ,  $i = 1, 2$ , is a geometry parameter vector of the  $i$ th cells,  $\beta$  is a penalty factor (here, we use  $\beta = 10^4$ ), whereas  $S_{11.i}(\mathbf{x}_i; f)$  and  $S_{21.i}(\mathbf{x}_i; f)$  denote explicit dependence of  $S$ -parameters on frequency for the  $i$ th cell. Therefore, the process (3) aims at minimizing  $|S_{11}|$  in the vicinity of  $f_0$  (in practice, at three frequency points:  $f_0 - df$ ,  $f_0$ , and  $f_0 + df$ ), while forcing  $\arg(S_{21})$  to obtain the value of  $\phi_c$ . The value of  $\beta$  is set to ensure that even small violation of the phase requirement results in a meaningful contribution of the penalty function. Here, for  $\beta = 10^4$ , deviation of  $\arg(S_{21.i})$  from  $\phi_c$  by  $0.01^\circ$  results in the penalty function value of 1, which is a few percent of the primary cost function value; for deviation by  $0.1^\circ$ , the penalty function becomes a dominant component of  $U$ . Thus, formulation (4) allows for obtaining the required phase shift with good accuracy. The use of three frequency points is motivated by the necessity of ensuring an adequate reflection response not only at the operating frequency but also in some vicinity of it. Moreover, minimization of (4) leads to obtaining more or less symmetric response around  $f_0$  with  $|S_{11}|$  being equal (or almost equal) at both  $f_0 - df$  and  $f_0 + df$ . The problem (3) is solved using a pattern search algorithm (cf. [33]).

### 4.2.3 Response Surface Approximation (RSA) Models

Local RSA models of the non-uniform building blocks of a compact BLC, exploited during the fine-tuning process (cf. Sect. 4.2.4), are developed in the neighborhood of their optimized designs,  $\mathbf{x}_{c,i}^*$ ,  $i = 1, 2$ , defined as  $[\mathbf{x}_{c,i}^* - d\mathbf{x}_i, \mathbf{x}_{c,i}^* + d\mathbf{x}_i]$ . Each model uses  $2n_i + 1$  ( $n_i = \dim(\mathbf{x}_i)$ ) EM simulations for each composite cell at  $\mathbf{x}_{c,i}^{(0)} = \mathbf{x}_{c,i}^*$  and at the perturbed designs  $\mathbf{x}_{c,i}^{(k)} = [\mathbf{x}_{c,i,1}^* \dots \mathbf{x}_{c,i,[k/2]}^* + (-1)^k d\mathbf{x}_{i,[k/2]} \dots \mathbf{x}_{c,i,n_i}^*]^T$ ,  $k = 1, \dots, 2n_i$ , where  $\mathbf{x}_{c,i,k}^*$  and  $d\mathbf{x}_{i,k}$  are  $k$ th elements of the vectors  $\mathbf{x}_{c,i}^*$  and  $d\mathbf{x}_i$ , respectively. The RSA model  $\mathbf{R}_{c,i}(\mathbf{x})$  of the  $i$ th cell is a simple second-order polynomial without mixed terms

$$\mathbf{R}_{c,i}(\mathbf{x}) = c_{0,i} + \sum_{k=1}^{n_i} c_{k,i} x_{i,k} + \sum_{k=1}^{n_i} c_{(n+k),i} x_{i,k}^2 \quad (5)$$

with the parameters determined as least-square solution to the linear regression problem  $\mathbf{R}_{c,i}(\mathbf{x}_{c,i}^{(k)}) = \mathbf{R}_{f,i}(\mathbf{x}_{c,i}^{(k)})$ ,  $k = 0, 1, \dots, 2n_i$ , where  $\mathbf{R}_{f,i}$  denotes the EM model of the  $i$ th non-uniform building block of a compact BLC. The RSA model  $\mathbf{R}_c$  of the entire coupler is subsequently constructed by cascading  $\mathbf{R}_{c,i}$  using ABCD matrix representation [1]. The particular choice of the RSA model comes from the fact that  $S$ -parameters of the individual cells are not highly nonlinear (the modeling is carried out for complex responses), and the model needs to be valid only in the vicinities of the optimized cell geometries.

### 4.2.4 Surrogate-Assisted Design Refinement

In order to account for cross-coupling effects between the adjacent BLC building blocks, as well as other phenomena (e.g., T-junction phase shifts), it is required to perform a final fine-tuning of the entire BLC. The tuning procedure is realized as a surrogate-based optimization process

$$\mathbf{x}^{(i+1)} = \arg \min_{\mathbf{x}} H(\mathbf{R}_s^{(i)}(\mathbf{x})) \quad (6)$$

Vectors  $\mathbf{x}^{(i)}$ ,  $i = 0, 1, \dots$ , approximate the solution of the direct design problem  $\mathbf{x}^* = \operatorname{argmin}\{\mathbf{x} : H(\mathbf{R}_f(\mathbf{x}))\}$  ( $H$  encodes design specifications for the coupler), whereas  $\mathbf{R}_s^{(i)}$  is the surrogate model at iteration  $i$ .  $\mathbf{R}_s^{(i)}$  is constructed from the RSA model  $\mathbf{R}_c$  using input space mapping [42]

$$\mathbf{R}_s^{(i)}(\mathbf{x}) = \mathbf{R}_c(\mathbf{x} + \mathbf{q}^{(i)}) \quad (7)$$

where  $\mathbf{q}^{(i)}$  is the input SM shift vector acquired through the usual parameter extraction procedure  $\mathbf{q}^{(i)} = \operatorname{argmin}\{\mathbf{q} : \|\mathbf{R}_f(\mathbf{x}^{(i)}) - \mathbf{R}_c(\mathbf{x}^{(i)} + \mathbf{q})\|\}$ , aiming at minimization of misalignment between the  $\mathbf{R}_c$  and the EM model  $\mathbf{R}_f$  of the structure under consideration. Upon completion of parameter extraction, the surrogate model becomes a very good representation of the high-fidelity model in the vicinity of the current

design so that it can be successfully used to find the optimum design of the latter. Note that the high-fidelity model  $\mathbf{R}_f$  is not evaluated until the fine-tuning stage. In practice, a single iteration (6) is sufficient. The overall cost of the coupler design process is therefore very low and usually corresponds to a few simulations of the entire structure of interest, including cell optimization and the cost associated with the development of the RSA models.

### 4.3 Results

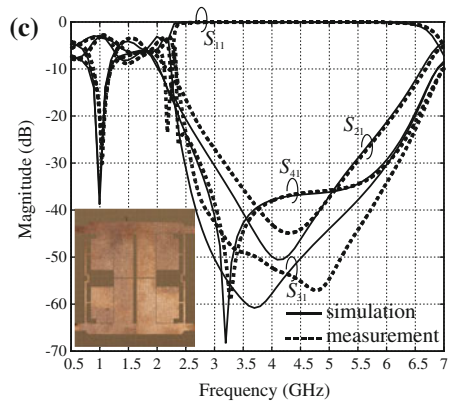
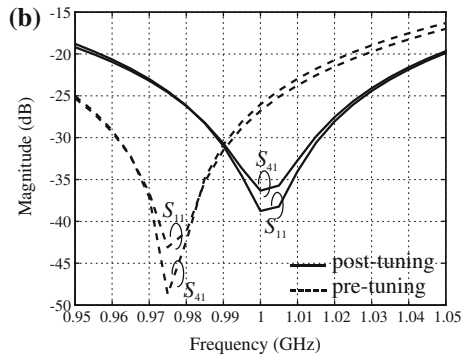
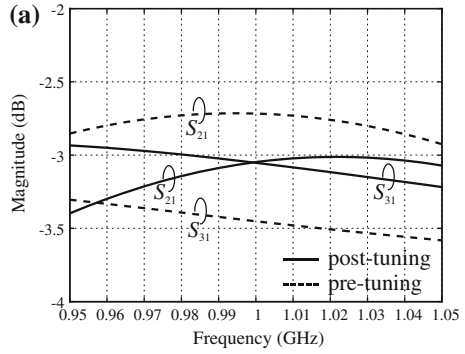
Here, we use Sonnet *em* [96] to conduct all high-fidelity EM simulations, where the grid size is set to  $0.025 \text{ mm} \times 0.0025 \text{ mm}$  to provide sufficient accuracy of composite cell design solutions. EM simulations are performed on PC with 8-core Intel Xeon 2.5 GHz processor and 6 GB RAM. With this setup, single frequency simulation of an individual non-uniform building block of a compact BLC is, on average, 15 and 18 s. Simulation time of the entire BLC is approximately 90 min.

First, we perform concurrent optimization of the cells of Fig. 2. Design requirements, imposed on each constitutive cell, are theory-based [80]. Therefore we aim at finding appropriate cell designs that approximate electrical parameters of theoretical BLC building blocks. More specifically,  $|S_{11}| \leq -20 \text{ dB}$  at 0.96, 1, and 1.04 GHz, when loaded with  $35.35 \Omega$  and  $50 \Omega$  resistances, respectively, and the phase shift  $\phi_c = -90^\circ$  at  $f_0$ . Both cells of Fig. 2 have been subjected to concurrent optimization, yielding  $\mathbf{x}_c^* = [0.45 \ 1.9 \ 3.325 \ 0.225 \ 1.55 \ 0.125 \ 8.05 \ 0.1 \ 1.15 \ 0.1 \ 0.41]^T$ . Corresponding constrained optima for individual cells are  $f_1(\mathbf{x}_c^*) = [0.45 \ 1.9 \ 3.325 \ 0.225 \ 1.55 \ 0.125 \ 8.05]^T \text{ mm}$ , and  $f_2(\mathbf{x}_c^*) = [0.1 \ 1.15 \ 0.1 \ 0.4 \ 1 \ 2.675 \ 2.925 \ 0.9]^T \text{ mm}$ . The EM evaluation of the entire coupler structure at the design produced in this step illustrates a degraded performance due to cross-coupling effects that occur between adjacent cells. This issue is addressed by the fine-tuning procedure. For that purpose, we develop local RSA models of the respective optimized cells and use them to construct the coarse model of the entire coupler (by cascading ABCD matrices of the corresponding building blocks). Next, we execute the surrogate-assisted design refinement algorithm.

The differences between pre- and post-tuning coupler design solution are depicted in Fig. 4a, b. One can notice that the final post-tuning BLC, given by  $f_1(\mathbf{x}^*) = [0.475 \ 1.9 \ 3.25 \ 0.225 \ 1.5 \ 0.125 \ 8.05]^T \text{ mm}$ , and  $f_2(\mathbf{x}^*) = [0.125 \ 1.15 \ 0.125 \ 0.375 \ 0.95 \ 2.7 \ 2.925 \ 0.875]^T \text{ mm}$ , shows perfect transmission characteristics in contradiction to the pre-tuning BLC design. The final design solution has been manufactured and measured.

Measurement results presented in Fig. 4c are in agreement with the simulated BLC performance. Minor discrepancy between simulation and measurement results is most likely due to the smooth metal surface and dielectric anisotropy included in EM simulation [97], as well as fabrication inaccuracy.

**Fig. 4 a–b** pre-tuning (dashed) versus post-tuning (solid) BLC S-parameters; **c** post-tuning BLC broadband performance—simulation versus measurement



It should be emphasized that the final BLC has reached a significant 83.7% scale of miniaturization in comparison to a conventional BLC, together with ideal characteristics confirmed by measurement data—all at a low computational cost corresponding to about 5.6 full-wave analyses of the final compact BLC high-fidelity EM model. The design cost breakdown is as follows: concurrent cell optimization (150 cell evaluations at three frequencies each,  $\sim 225$  min in total), simulation data for RSA model construction (21 cell evaluations at 10 frequencies each,  $\sim 105$  min in total), and two simulations of the entire coupler ( $\sim 180$  min). The overall design cost of the proposed method is  $\sim 510$  min. One should bear in mind that a direct optimization would require several hundred such evaluations, which is virtually infeasible.

## 5 Case Study II: Fast Design of Compact RF Circuits Using Nested Space Mapping

Design and optimization of microwave/RF circuits for space limited applications is a challenging task. Miniaturization of a structure is usually obtained by replacing its fundamental building blocks with composite elements that should be adjusted to obtain compact geometry [6, 7]. Unfortunately, implementation of such elements within a circuit significantly increases its complexity, and therefore a considerable amount of simulations is needed to find the optimum design. Consequently, direct utilization of high-fidelity EM simulations in the design process is usually prohibitive. This issue can be partially resolved by using equivalent circuit representations of the structure which are, however, of limited accuracy [2, 10]. In this section, we discuss a so-called nested space mapping (NSM) methodology that aims at using suitably corrected circuit models as well as structure decomposition for fast EM-driven design of compact microwave structures. NSM provides two levels of structure representation, i.e., inner- and outer-layer surrogate models. The former is applied at the level of each sub-circuit in order to provide their good generalization capability. The latter is utilized at the level of entire complex design to account for couplings between sub-circuits.

### 5.1 Design Problem and Matching Transformer Structure

Consider a impedance transformer realized in microstrip technology aimed to match 50-Ohm source to 130-Ohm load. The structure is supposed to ensure reflection  $|S_{11}| \leq -15$  dB within 3.1 GHz to 10.6 GHz frequency. A circuit is designated to operate on a Taconic RF-35 dielectric substrate ( $\epsilon_r = 3.5$ ,  $\tan\delta = 0.0018$ ,  $h = 0.762$ ).

A conventional design that is sufficient to satisfy the aforementioned design specifications is composed of four  $90^\circ$  transmission line sections of various impedances [1]. The geometry of a structure and its circuit representation with highlighted sections



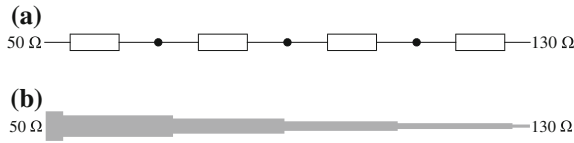


**Fig. 5** Conventional 50-Ohm to 130-Ohm matching transformer: **a** circuit representation; **b** geometry of a structure

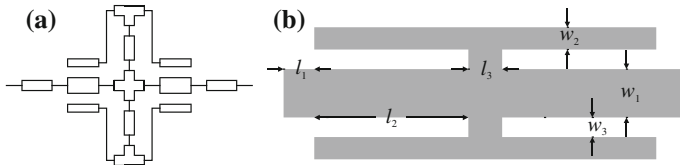


**Fig. 6** A double-T composite structure: **a** circuit representation; **b** geometry with highlighted dimensions

are illustrated in Fig. 5. The simplicity of the design allows for its decomposition into four transmission line sections that could be substituted with composite elements of increased functionality [2]. A single, versatile component in the form of double-T composite may be utilized to construct miniaturized matching transformer [98]. The structure of interest is described by four independent design parameters:  $\mathbf{y} = [l_1 \ l_2 \ w_1 \ w_2]^T$  (variables  $l_3 = 0.2$  and  $w_3 = 0.2$  are fixed). Moreover, solution space for the component in the form of the following lower/upper  $\mathbf{l}/\mathbf{u}$  bounds:  $\mathbf{l} = [0.1 \ 1 \ 0.1 \ 0.1]^T$  and  $\mathbf{u} = [1 \ 5 \ 1 \ 1]^T$  is defined to account for technology limitations (i.e., minimum feasible width of the composite element lines and the gaps between them equal to 0.1 mm). A high-fidelity model of the double-T composite element ( $\sim 200,000$  mesh cells and average evaluation time of 60 s) is implemented in CST Microwave Studio [39], whereas its circuit representation is constructed in Agilent ADS simulator [99]. Figure 6 illustrates a circuit and EM model of a double-T composite structure.

### 5.2 Optimization Methodology

Let  $\mathbf{y}$  stand for the geometry parameters of a composite element, whereas  $\mathbf{R}_{f,cell}(\mathbf{y})$  and  $\mathbf{R}_{c,cell}(\mathbf{y})$  denote the responses of EM and circuit models, respectively. The nested space mapping method [25, 98] constructs a surrogate model of a miniaturized structure starting from the level of each composite element (a so-called local level space mapping). Consider  $\mathbf{R}_{s,g,cell}(\mathbf{y}, \mathbf{p})$  as a generic surrogate model, constructed using  $\mathbf{R}_{c,cell}$  and suitable space mapping transformations. Vector  $\mathbf{p}$  denotes extractable space mapping parameters of the surrogate. The  $\mathbf{R}_{s,cell}$  model is obtained using the following transformation

$$\mathbf{R}_{s.cell}(\mathbf{y}) = \mathbf{R}_{s.g.cell}(\mathbf{y}, \mathbf{p}^*) \quad (8)$$

where

$$\mathbf{p}^* = \arg \min_{\mathbf{p}} \sum_{k=1}^{N_{cell}} \|\mathbf{R}_{s.g.cell}(\mathbf{y}^{(k)}, \mathbf{p}) - \mathbf{R}_f(\mathbf{y}^{(k)})\| \quad (9)$$

Here,  $\mathbf{y}^{(k)}$ ,  $k = 1, \dots, N_{cell}$ , are the training designs obtained using a star-distribution scheme. The base set is composed of  $N_{cell} = 2n + 1$ , where  $n$  is a number of independent design variables. A surrogate model  $\mathbf{R}_{s.g.cell}$  is usually constructed using a combination of input SM, implicit SM and frequency scaling [24] in such a way that  $\mathbf{R}_{s.cell}$  is accurate within entire solution space of the model.

Let  $\mathbf{R}_f(\mathbf{x})$  and  $\mathbf{R}_c(\mathbf{x})$  denote the EM and circuit models of the entire composite structure with  $\mathbf{x}$  being a vector of geometry parameters. Additionally, let  $\mathbf{R}_{s.g}(\mathbf{x}, \mathbf{P})$  stand for a surrogate model of the entire compact structure, constructed of surrogate models of composite elements, i.e.,  $\mathbf{R}_{s.g}(\mathbf{x}, \mathbf{P}) = \mathbf{R}_{s.g}([\mathbf{y}_1; \dots; \mathbf{y}_p], \mathbf{P}) = F(\mathbf{R}_{s.g.cell}(\mathbf{y}_1, \mathbf{p}^*), \dots, \mathbf{R}_{s.g.cell}(\mathbf{y}_p, \mathbf{p}^*), \mathbf{P})$ . Function  $F$  realizes a cascade connection of individual composite element responses [2, 98], whereas the vector  $\mathbf{x}$  is a concatenation of component parameter vectors  $\mathbf{y}_k$  (where  $k = 1, \dots, p$ ). The outer layer surrogate model parameter vector  $\mathbf{P}$  is usually defined as a perturbation with respect to selected space mapping parameters  $\mathbf{p}^*$  of each composite element.

An outer space mapping correction is applied at the level of entire compact structure  $\mathbf{R}_{s.g}(\mathbf{x}, \mathbf{P})$ , so that the final surrogate  $\mathbf{R}_s^{(i)}$  utilized in the  $i$ th iteration of the surrogate-based optimization scheme (2) is as follows

$$\mathbf{R}_s^{(i)}(\mathbf{x}) = \mathbf{R}_{s.g}(\mathbf{x}^{(i)}, \mathbf{P}^{(i)}) \quad (10)$$

where

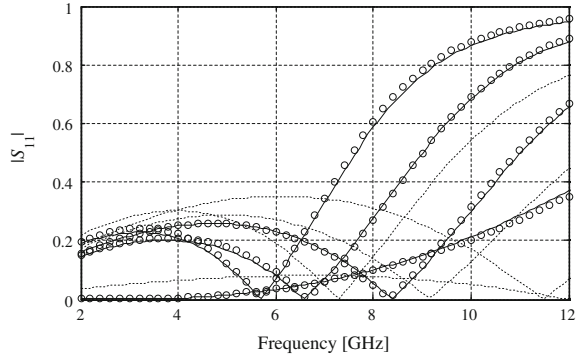
$$\mathbf{P}^{(i)} = \arg \min_{\mathbf{P}} \|\mathbf{R}_{s.g}(\mathbf{x}^{(i)}, \mathbf{P}) - \mathbf{R}_f(\mathbf{x}^{(i)})\| \quad (11)$$

Generally, vector  $\mathbf{P}$  utilized in NSM approach is composed of considerably smaller number of space mapping parameters than in competitive techniques, which is due to good alignment of  $\mathbf{R}_{s.cell}$  and  $\mathbf{R}_{f.cell}$  provided by the inner SM layer. For more detailed description of nested space mapping methodology see e.g. [25, 98].

### 5.3 Results

For demonstration purposes, a compact 50-Ohm to 130-Ohm impedance transformer composed of a cascade connected double-T composite elements [98] is considered for optimization with respect to the design specifications of Sect. 5.1. A surrogate model  $\mathbf{R}_{s.cell}$  is constructed using a total of 16 space mapping parameters including: 8 input space mapping, 6 implicit space mapping, and 2 frequency scaling ones [25, 41, 92]. Subsequently, a 9-point parameter extraction based on star-distribution

**Fig. 7** Responses of double-T composite element at the selected test designs: coarse model (⋯⋯), fine model (—), NSM surrogate after multipoint parameter extraction (○ ○ ○). The plots indicate very good approximation capability of the surrogate



scheme is performed. Figure 7 illustrates a comparison of the model responses before and after multi-point parameter extraction step.

An outer layer surrogate model  $R_{s.g}$  of the compact matching transformer is composed of interconnected surrogate models of composite elements  $R_{s.cell}$ . Its corresponding  $R_f$  counterpart is prepared in CST Microwave Studio (~1,060,000 mesh cells and average simulation time of 10 min). The initial set of design parameters is:  $x = [0.55 \ 3.75 \ 0.65 \ 0.35 \ 0.55 \ 3.75 \ 0.65 \ 0.35 \ 0.55 \ 3.75 \ 0.65 \ 0.35 \ 0.55 \ 3.75 \ 0.65 \ 0.35]^T$ . Next, the NSM technique of Sect. 5.2 is utilized to obtain the final design. Optimized compact matching transformer is represented by the following vector of design parameters:  $x = [1.0 \ 3.52 \ 0.85 \ 0.2 \ 0.8 \ 4.1 \ 0.58 \ 0.1 \ 0.8 \ 3.09 \ 0.1 \ 0.25 \ 1 \ 2.32 \ 0.13 \ 0.1]^T$ . Schematic representation of  $R_s$  model of compact structure in the form of cascade connection of  $R_{s.cell}$  models and geometry of a circuit are illustrated in Fig. 8.

The optimized design that satisfies all assumed requirements, i.e., provides 50-Ohm source to 130-Ohm load matching and  $|S_{11}| \leq -15$  dB within defined oper-

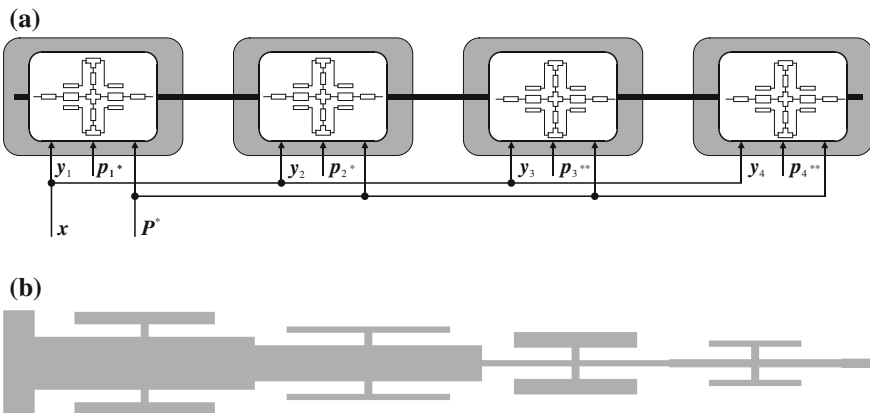
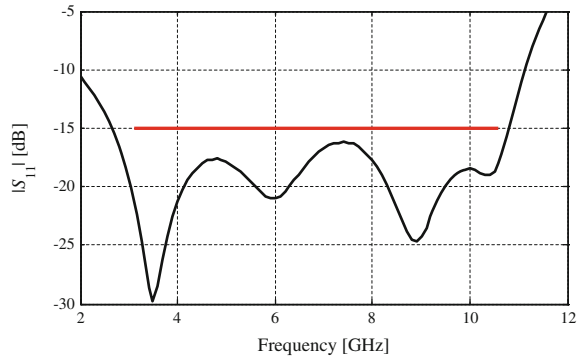


**Fig. 8** A compact matching transformer: **a** schematic diagram of double-T composite element interconnections; **b** geometry of an optimized structure

**Fig. 9** Reflection response of the optimized compact matching transformer



ational bandwidth is obtained after only 3 iterations of nested space mapping algorithm. One should note that the optimized structure exhibits 15 % broader bandwidth than the assumed (lower and upper operating frequency is 2.7 GHz and 10.8 GHz, respectively). Moreover, reflection level for 3.1 GHz to 10.6 GHz bandwidth is below  $-16.2$  dB, which is almost 15 % lower than the assumed value. Reflection characteristic of the optimized design is shown in Fig. 9.

The total cost of compact matching transformer design and optimization is about 40 min and it includes: 9 simulations of  $\mathbf{R}_{f,cell}$  model during multi-point parameter extraction, 3 evaluations of the  $\mathbf{R}_f$  model, and simulations of surrogate models that corresponds to a total of  $0.2 \mathbf{R}_f$ . It should be emphasized that NSM technique outclasses other competitive methods, i.e., implicit space mapping [100], and sequential space mapping [2]. The results indicate that the computational cost of the method is almost 70 % smaller in comparison to implicit space mapping and sequential space mapping. For the sake of comparison, a direct optimization driven by pattern search algorithm [33] has been also conducted; however algorithm failed to find a design satisfying given specifications and it was terminated after 500 iterations. Table 1 gathers detailed data concerning the computational cost of techniques utilized for transformer optimization.

**Table 1** Four section unconventional MT: design and optimization cost

Model type	Optimization algorithm			
	NSM	ISM	SSM	Direct search
$\mathbf{R}_{s,cell}$	$0.1 \times \mathbf{R}_f$	N/A	N/A	N/A
$\mathbf{R}_{f,cell}$	$0.6 \times \mathbf{R}_f$	N/A	N/A	N/A
$\mathbf{R}_s$	$0.1 \times \mathbf{R}_f$	$5.1 \times \mathbf{R}_f$	$1.7 \times \mathbf{R}_f$	N/A
$\mathbf{R}_f$	3	7	$10^a$	$500^b$
Total cost	$3.8 \times \mathbf{R}_f$	$12.1 \times \mathbf{R}_f$	$11.7 \times \mathbf{R}_f$	$500^b \times \mathbf{R}_f$
Total cost [min]	38	121	N/A	5000

<sup>a</sup>The algorithm started diverging and was terminated after 10 iterations

<sup>b</sup>The algorithm failed to find a geometry satisfying performance specifications

## 6 Case Study III: Simulation-Driven Design of Small UWB Antennas

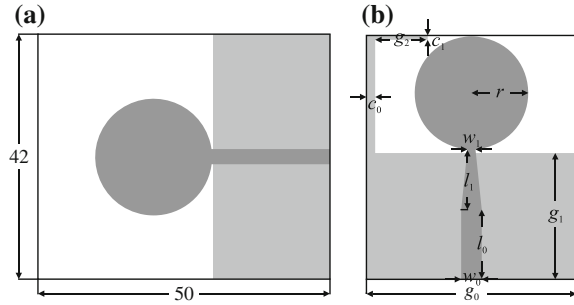
Antennas are crucial components in mobile communication systems. They play a role of an interface between the wireless medium and the transmission lines. Ultra-wideband (UWB) antennas are of particular interest, because they can provide high data transmission rates, and their broadband properties could be useful for reduction of transceiver section complexity [28]. On the other hand, such antennas are characterized by considerable footprint, which is a serious drawback: rapid development of handheld devices imposes strict requirements upon miniaturization of contemporary antenna structures. Miniaturization of ultra-wideband antennas is troublesome, since their performance—especially for lower frequency range—depends on the wideband impedance and current path within the ground plane [28]. While the former may be accounted for by appropriate construction of the feeding line, the latter requires complex modifications within the ground plane. Unintuitive and asymmetrical geometries of compact UWB antennas significantly influence the evaluation cost of their EM models, which varies from half an hour up to several hours. These problems make the design and optimization of compact ultra-wideband antennas a challenging task. In particular, their simulation-driven design directly based on high-fidelity EM models is impractical [84]. On the other hand, lack of theoretical insight for such structures makes EM simulators the only reliable tools for their performance evaluation. In this section, a design of compact UWB antenna with modified ground plane and feed line is discussed. Computational efficiency of the optimization process is ensured by the utilization of high- and low-fidelity EM models. Discrepancy between model responses is addressed using adaptively-adjusted design specification (AADS) technique [85].

### 6.1 Antenna Structure and Design Problem

Consider a conventional planar monopole antenna [101] consisting a circular shape radiator and a feeding structure in the form of 50-Ohm microstrip line. The structure is characterized by a considerable size of  $45 \times 50 \text{ mm}^2$ , which is necessary to achieve wideband impedance matching and sufficient current path within ground plane. The structure can be miniaturized by introduction of a tapered feed line and modification of the ground plane by means of a L-shaped ground plane stub [102, 103]. Geometry of a conventional monopole and its compact counterpart with modified geometry is illustrated in Fig. 10.

The antenna is described by seven independent design variables:  $\mathbf{x} = [g_0 \ g_1 \ l_1 \ r g_2 \ c_0 \ w_1]^T$ , whereas  $w_0 = 2.35$ ,  $l_0 = 8$  remain fixed;  $c_1 = c_0/2$  (all dimensions in mm). It is designated to work on Taconic TLP-5 dielectric substrate ( $\epsilon_r = 2.2$ ,  $\tan\delta = 0.0009$ ,  $h = 0.762$  mm). In order to utilize AADS methodology for the design and optimization, two models of an antenna have been prepared

**Fig. 10** Monopole UWB antenna: **a** initial design [101]; **b** a compact structure with modified geometry [28]



and simulated in CST Microwave Studio transient solver. The high-fidelity model  $\mathbf{R}_f$  is represented by  $\sim 2,577,000$  mesh cells and average evaluation time of 30 min, whereas its low-fidelity counterpart  $\mathbf{R}_c$  is composed of  $\sim 75,000$  mesh cells and its average simulation time is 47 s.

Two design cases are considered: (i) reduction of antenna footprint defined as a rectangle  $R = A \times B$ , where  $A = g_0$  and  $B = l_0 + l_1 + 2r$ , and (ii) minimization of antenna reflection. One should note that operational properties of an antenna optimized within the former criteria, i.e.,  $|S_{11}| \leq -10$  dB are enforced by sufficiently defined penalty factor. Both objectives are considered within 3.1 GHz to 10.6 GHz frequency band.

## 6.2 Optimization Methodology

In order to provide reliable prediction of the antenna response, a misalignment between  $\mathbf{R}_f$  and  $\mathbf{R}_c$  responses is accounted for by means of adaptively adjusted design specifications (AADS) technique [85]. Majority of available surrogate-based optimization techniques (e.g., [22, 56, 100]) perform enhancement and corrections of the  $\mathbf{R}_c$  model in order to minimize its misalignment with respect to  $\mathbf{R}_f$ . The AADS methodology utilizes knowledge about discrepancy between responses of  $\mathbf{R}_c$  and  $\mathbf{R}_f$  in order to modify design specifications so that they account for the response differences. AADS works very well for a problems that are defined in a minimax sense, e.g.,  $|S_{11}| \leq -10$  dB over a defined operational frequency, which is the case for the design of UWB antenna structures. A conceptual explanation of the method with highlight on the determination of characteristic points is provided in Fig. 11, whereas the algorithm flow is presented below:

1. Modify the original design specifications to account for the difference between the responses of  $\mathbf{R}_f$  and  $\mathbf{R}_c$  at their characteristic points.
2. Obtain a new design by optimizing the low-fidelity model  $\mathbf{R}_c$  with respect to the modified specifications.

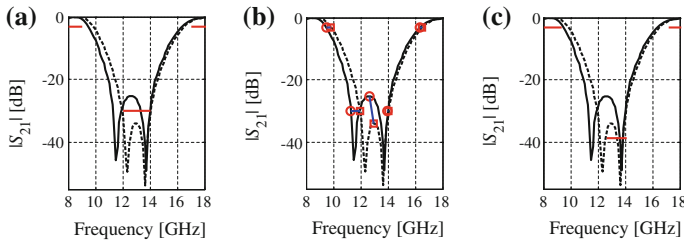


**Fig. 11** Design optimization through AADS [85] on the basis of a bandstop filter  $R_f$  (—) and  $R_c$  (- - -): **a** initial responses and the original design specifications, **b** characteristic points of the responses corresponding to the specification levels (here,  $-3$  and  $-30$  dB) and to the local maxima, **c** responses at the initial design as well as the modified design specifications. The modification accounts for the discrepancy between the models: optimizing  $R_c$  w.r.t. the modified specs corresponds (approximately) to optimizing  $R_f$  w.r.t. the original specs

In the first step of algorithm, the specifications are altered in such a way that specifications for  $R_c$  model corresponds to the desired frequency properties of the high fidelity one. In the second stage, the  $R_c$  model is optimized with respect to the redefined design specifications. The optimal design is an approximated solution to the original problem defined for  $R_f$  model. Although the most considerable design improvement is normally observed after the first iteration, the algorithm steps may be repeated if further refinement of design specifications is required. In practice, the algorithm is terminated once the current iteration does not bring further improvement of the high-fidelity model design. One should emphasize that determination of appropriate characteristic points is crucial for the operation of the technique. They should account for local extrema of both model responses, at which specifications may not be satisfied. Moreover, due to differences between  $R_f$  and  $R_c$  models, redefinition of design specifications may be necessary at each algorithm iteration.

### 6.3 Results

The initial design of a compact monopole antenna of Sect. 6.1 is  $\mathbf{x}^0 = [24 \ 14.5 \ 7 \ 6.5 \ 6 \ 1 \ 0.9]^T$  and corresponding footprint of a structure is  $672 \text{ mm}^2$ , whereas its maximal reflection within frequency band of interest is  $-10.8$  dB. The design parameters of a structure optimized with respect to minimization of reflection are  $\mathbf{x}^{(i)} = [26.58 \ 13.83 \ 6.19 \ 6.24 \ 7.79 \ 0.330 \ 0.7]^T$ . The design is obtained after 3 iterations of the AADS algorithm. The second design—optimized towards minimization of footprint—has been obtained after only 2 iterations of the algorithm and the corresponding dimensions are  $\mathbf{x}^{(ii)} = [19.78 \ 13.63 \ 5.81 \ 5.84 \ 7.89 \ 0.33 \ 0.72]^T$ . The footprint of a structure is only  $504 \text{ mm}^2$ . It should be emphasized that the design optimized with respect to reflection is characterized by a maximal in-band  $|S_{11}| = -13.5$  dB which is 20% lower in comparison with the reference structure. Additionally, the

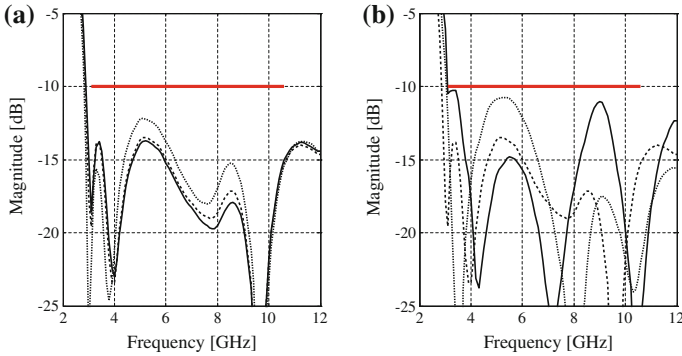


**Fig. 12** Reflection response of optimized compact UWB monopole antennas. Initial design ( $\cdot \cdot \cdot$ ), first iteration ( $- - -$ ), final result ( $—$ ): **a** design (i); **b** design (ii)

**Table 2** Design of a compact UWB antenna: optimization results

Antenna design	AADS		Direct-search (pattern search)	
	Design (i)	Design (ii)	Design (i)	Design (ii)
$R_c$	300	200	N/A	N/A
$R_f$	4	3	97	107
Total cost	$11.8 \times R_f$	$8.2 \times R_f$	$97 \times R_f$	$107 \times R_f$
Total cost [h]	5.9	4.1	48.5	53.5

antenna optimized with respect to minimization of the lateral area is 25% smaller than the reference one. It should be also highlighted that the variation of size between both optimized structures is 29%, whereas their maximal in-band reflection varies by 26%. Frequency responses of both optimized antenna designs are shown in Fig. 12.

The optimization cost for the first case corresponds to  $11.8 R_f$  ( $\sim 5.9$  h) and it includes: a total of  $300 R_c$  evaluations for the design optimization and  $4 R_f$  simulations for the response verification. The cost of obtaining the second design corresponds to about  $8.2 R_f$  model simulations ( $\sim 4.1$  h):  $200 R_c$  simulations for the design optimization and  $3 R_f$  model evaluations. For the sake of comparison, both designs have been optimized using direct-search approach driven by pattern search algorithm [33]. The cost of design optimization towards minimum reflection and footprint miniaturization is  $97 R_f$  and  $107 R_f$ , respectively. Design costs for these two cases are over 8 and over 13 times lower compared to direct search. A detailed comparison of design and optimization cost of both designs is gathered in Table 2.



## 7 Conclusion

This chapter highlighted several techniques for rapid EM-simulation-driven design of miniaturized microwave and antenna structures. Techniques such as nested space mapping, design tuning exploiting structure decomposition and local approximation models, or adaptively adjusted design specifications, can be utilized to obtain the optimized geometries of compact circuits in reasonable timeframe. The key is a proper combination of fast low-fidelity models, their suitable correction, as well as appropriate correction-prediction schemes linking the process of surrogate model identification and optimization. In all of the discussed schemes, the original, high-fidelity model is referred to rarely (for design verification and providing data for further surrogate model enhancement). In case of compact microwave structures, it is also usually possible to exploit structure decomposition, which further speeds up the design process. In any case, it seems that tailoring the optimization method for a given design problems gives better results than taking off-the-shelf algorithm. One of the open problems in the field discussed in this chapter include design automation, such as automated selection of the low-fidelity model, as well as controlling the convergence of the surrogate-based optimization process. This and other issues will be the subject of the future research.

## References

1. Pozar, D.M.: *Microwave Engineering*, 4th edn. Wiley, Hoboken (2012)
2. Bekasiewicz, A., Kurgan, P., Kitlinski, M.: A new approach to a fast and accurate design of microwave circuits with complex topologies. *IET Microw. Antennas Propag.* **6**, 1616–1622 (2012)
3. Smierzchalski, M., Kurgan, P., Kitlinski, M.: Improved selectivity compact band-stop filter with Gosper fractal-shaped defected ground structures. *Microw. Opt. Technol. Lett.* **52**, 227–232 (2010)
4. Kurgan, P., Kitlinski, M.: Novel microstrip low-pass filters with fractal defected ground structures. *Microw. Opt. Technol. Lett.* **51**, 2473–2477 (2009)
5. Aznar, F., Velez, A., Duran-Sindreu, M., Bonache, J., Martin, F.: Elliptic-function CPW low-pass filters implemented by means of open complementary split ring resonators (OCSRRs). *IEEE Microw. Wirel. Compon. Lett.* **19**, 689–691 (2009)
6. Kurgan, P., Bekasiewicz, A., Pietras, M., Kitlinski, M.: Novel topology of compact coplanar waveguide resonant cell low-pass filter. *Microw. Opt. Technol. Lett.* **54**, 732–735 (2012)
7. Bekasiewicz, A., Kurgan, P.: A compact microstrip rat-race coupler constituted by nonuniform transmission lines. *Microw. Opt. Technol. Lett.* **56**, 970–974 (2014)
8. Opozda, S., Kurgan, P., Kitlinski, M.: A compact seven-section rat-race hybrid coupler incorporating PBG cells. *Microw. Opt. Technol. Lett.* **51**, 2910–2913 (2009)
9. Kurgan, P., Kitlinski, M.: Novel doubly perforated broadband microstrip branch-line couplers. *Microw. Opt. Technol. Lett.* **51**, 2149–2152 (2009)
10. Kurgan, P., Bekasiewicz, A.: A robust design of a numerically demanding compact rat-race coupler. *Microw. Opt. Technol. Lett.* **56**, 1259–1263 (2014)
11. Wu, Y., Liu, Y., Xue, Q., Li, S., Yu, C.: Analytical design method of multiway dual-band planar power dividers with arbitrary power division. *IEEE Trans. Microw. Theory Tech.* **58**, 3832–3841 (2010)

12. Chiu, L., Xue, Q.: A parallel-strip ring power divider with high isolation and arbitrary power-dividing ratio. *IEEE Trans. Microw. Theory Tech.* **55**, 2419–2426 (2007)
13. Bekasiewicz, A., Koziel, S., Ogurtsov, S., Zieniutycz, W.: Design of microstrip antenna subarrays: a simulation-driven surrogate-based approach. In: *International Conference Microwaves, Radar and Wireless Communications* (2014)
14. Wang, X., Wu, K.-L., Yin, W.-Y.: A compact gysel power divider with unequal power-dividing ratio using one resistor. *IEEE Trans. Microw. Theory Tech.* **62**, 1480–1486 (2014)
15. Koziel, S., Ogurtsov, S., Zieniutycz, W., Bekasiewicz, A.: Design of a planar UWB dipole antenna with an integrated balun using surrogate-based optimization. *IEEE Antennas Wirel. Propag. Lett.* (2014)
16. Shao, J., Fang, G., Ji, Y., Tan, K., Yin, H.: A novel compact tapered-slot antenna for GPR applications. *IEEE Antennas Wirel. Propag. Lett.* **12**, 972–975 (2013)
17. Koziel, S., Bekasiewicz, A.: Novel structure and EM-Driven design of small UWB monopole antenna. In: *International Symposium on Antenna Technology and Applied Electromagnetics* (2014)
18. Quan, X., Li, R., Cui, Y., Tentzeris, M.M.: Analysis and design of a compact dual-band directional antenna. *IEEE Antennas Wirel. Propag. Lett.* **11**, 547–550 (2012)
19. Koziel, S., Ogurtsov, S.: Multi-objective design of antennas using variable-fidelity simulations and surrogate models. *IEEE Trans. Antennas Propag.* **61**, 5931–5939 (2013)
20. Yeung, S.H., Man, K.F.: Multiobjective Optimization. *IEEE Microw. Mag.* **12**, 120–133 (2011)
21. Kuwahara, Y.: Multiobjective optimization design of Yagi-Uda antenna. *IEEE Trans. Antennas Propag.* **53**, 1984–1992 (2005)
22. Koziel, S., Bekasiewicz, A., Couckuyt, I., Dhaene, T.: Efficient multi-objective simulation-driven antenna design using Co-Kriging. *IEEE Trans. Antennas Propag.* **62**, 5900–5905 (2014)
23. Kurgan, P., Filipcewicz, J., Kitlinski, M.: Design considerations for compact microstrip resonant cells dedicated to efficient branch-line miniaturization. *Microw. Opt. Technol. Lett.* **54**, 1949–1954 (2012)
24. Bekasiewicz, A., Koziel, S., Pankiewicz, B.: Accelerated simulation-driven design optimization of compact couplers by means of two-level space mapping. *IET Microw. Antennas Propag.* (2014)
25. Koziel, S., Bekasiewicz, A., Kurgan, P.: Nested space mapping technique for design and optimization of complex microwave structures with enhanced functionality. In: Koziel, S., Leifsson, L., Yang, X.S. (eds.) *Solving Computationally Expensive Engineering Problems: Methods and Applications*, pp. 53–86. Springer, Switzerland (2014)
26. Kurgan, P., Bekasiewicz, A.: Atomistic surrogate-based optimization for simulation-driven design of computationally expensive microwave circuits with compact footprints. In: Koziel, S., Leifsson, L., Yang, X.S. (eds.) *Solving Computationally Expensive Engineering Problems: Methods and Applications*, pp. 195–218. Springer, Switzerland (2014)
27. Li, J.-F., Chu, Q.-X., Li, Z.-H., Xia, X.-X.: Compact dual band-notched UWB MIMO antenna with high isolation. *IEEE Trans. Antennas Propag.* **61**, 4759–4766 (2013)
28. Koziel, S., Bekasiewicz, A.: Small antenna design using surrogate-based optimization. In: *IEEE International Symposium on Antennas Propagation* (2014)
29. Liu, Y.-F., Wang, P., Qin, H.: Compact ACS-fed UWB monopole antenna with extra Bluetooth band. *Electron. Lett.* **50**, 1263–1264 (2014)
30. Koziel, S., Kurgan, P.: Low-cost optimization of compact branch-line couplers and its application to miniaturized Butler matrix design. In: *European Microwave Conference* (2014)
31. Nocedal, J., Wright, S.: *Numerical Optimization*, 2nd edn. Springer, New York (2006)
32. Koziel, S., Yang X.S. (eds.): *Computational optimization, methods and algorithms. Studies in Computational Intelligence*, vol. 356, Springer, New York (2011)
33. Kolda, T.G., Lewis, R.M., Torczon, V.: Optimization by direct search: new perspectives on some classical and modern methods. *SIAM Rev.* **45**, 385–482 (2003)
34. Deb, K.: *Multi-Objective Optimization Using Evolutionary Algorithms*. Wiley, Chichester (2001)
35. Talbi, E.-G.: *Metaheuristics—From Design to Implementation*. Wiley, Chichester (2009)

36. Koziel, S., Bekasiewicz, A., Zieniutycz, W.: Expedite EM-driven multi-objective antenna design in highly-dimensional parameter spaces. *IEEE Antennas Wirel. Propag. Lett.* **13**, 631–634 (2014)
37. Bekasiewicz, A., Koziel, S.: Efficient multi-fidelity design optimization of microwave filters using adjoint sensitivity. *Int. J. RF Microw. Comput. Aided Eng.* (2014)
38. Koziel, S., Ogurtsov, S., Cheng, Q.S., Bandler, J.W.: Rapid EM-based microwave design optimization exploiting shape-preserving response prediction and adjoint sensitivities. *IET Microw. Antennas Propag.* (2014)
39. CST Microwave Studio: CST AG, Bad Nauheimer Str. 19, D-64289 Darmstadt, Germany (2011)
40. Ansys HFSS: ver. 14.0, ANSYS, Inc., Southpointe 275 Technology Dr., Canonsburg, PA (2012)
41. Bandler, J.W., Cheng, Q.S., Dakroury, S.A., Mohamed, A.S., Bakr, M.H., Madsen, K., Sondergaard, J.: Space mapping: the state of the art. *IEEE Trans. Microw. Theory Tech.* **52**, 337–361 (2004)
42. Koziel, S., Bandler, J.W., Madsen, K.: Towards a rigorous formulation of the space mapping technique for engineering design. In: *Proceedings International Symposium Circuits and Systems* (2005)
43. Queipo, N.V., Haftka, R.T., Shyy, W., Goel, T., Vaidynathan, R., Tucker, P.K.: Surrogatebased analysis and optimization. *Prog. Aerosp. Sci.* **41**, 1–28 (2005)
44. El Zooghy, A.H., Christodoulou, C.G., Georgiopoulos, M.: A neural network-based smart antenna for multiple source tracking. *IEEE Trans. Antennas Propag.* **48**, 768–776 (2000)
45. Siah, E.S., Sasena, M., Volakis, J.L., Papalambros, P.Y., Wiese, R.W.: Fast parameter optimization of large-scale electromagnetic objects using DIRECT with Kriging metamodeling. *IEEE Trans. Microw. Theory Tech.* **52**, 276–285 (2004)
46. Xia, L., Meng, J., Xu, R., Yan, B., Guo, Y.: Modeling of 3-D vertical interconnect using support vector machine regression. *IEEE Microw. Wirel. Compon. Lett.* **16**, 639–641 (2006)
47. Kabir, H., Wang, Y., Yu, M., Zhang, Q.J.: Neural network inverse modeling and applications to microwave filter design. *IEEE Trans. Microw. Theory Tech.* **56**, 867–879 (2008)
48. Tighilt, Y., Bouttout, F., Khellaf, A.: Modeling and design of printed antennas using neural networks. *Int. J. RF Microw. Comput. Aided Eng.* **21**, 228–233 (2011)
49. Koziel, S., Bandler, J.W.: Space mapping with multiple coarse models for optimization of microwave components. *IEEE Microw. Wirel. Compon. Lett.* **18**, 1–3 (2008)
50. Koziel, S., Bandler, J.W., Cheng, Q.S.: Robust trust-region space-mapping algorithms for microwave design optimization. *IEEE Trans. Microw. Theory Tech.* **58**, 2166–2174 (2010)
51. Alexandrov, N.M., Lewis, R.M.: An overview of first-order model management for engineering optimization. *Optim. Eng.* **2**, 413–430 (2001)
52. Amineh, R.K., Koziel, S., Nikolova, N.K., Bandler, J.W., Reilly, J.P.: A space mapping methodology for defect characterization. In: *International Review of Progress in Applied Computational Electromagnetics* (2008)
53. Koziel, S., Bandler, J.W.: SMF: a user-friendly software engine for space-mapping-based engineering design optimization. In: *International Symposium Signals Systems Electronics* (2007)
54. Koziel, S., Leifsson, L., Ogurtsov, S.: Reliable EM-driven microwave design optimization using manifold mapping and adjoint sensitivity. *Microw. Opt. Technol. Lett.* **55**, 809–813 (2013)
55. Echeverria, D., Lahaye, D., Encica, L., Lomonova, E.A., Hemker, P.W., Vandenput, A.J.A.: Manifold-mapping optimization applied to linear actuator design. *IEEE Trans. Mangetics* **42**, 1183–1186 (2006)
56. Cheng, Q.S., Rautio, J.C., Bandler, J.W., Koziel, S.: Progress in simulator-based tuning—the art of tuning space mapping. *IEEE Microw. Mag.* **11**, 96–110 (2010)
57. Rautio, J.C.: Perfectly calibrated internal ports in EM analysis of planar circuits. In: *International Microwave Symposium Digest* (2008)

58. Gilmore, R., Besser, L.: *Practical RF Circuit Design for Modern Wireless Systems*. Artech House, Norwood (2003)
59. Xu, H.-X., Wang, G.-M., Lu, K.: Microstrip rat-race couplers. *IEEE Microw. Mag.* **12**, 117–129 (2011)
60. Ahn, H.-R., Bumman, K.: Toward integrated circuit size reduction. *IEEE Microw. Mag.* **9**, 65–75 (2008)
61. Liao, S.-S., Sun, P.-T., Chin, N.-C., Peng, J.-T.: A novel compact-size branch-line coupler. *IEEE Microw. Wirel. Compon. Lett.* **15**, 588–590 (2005)
62. Liao, S.-S., Peng, J.-T.: Compact planar microstrip branch-line couplers using the quasi-lumped elements approach with nonsymmetrical and symmetrical T-shaped structure. *IEEE Trans. Microw. Theory Tech.* **54**, 3508–3514 (2006)
63. Tang, C.-W., Chen, M.-G.: Synthesizing microstrip branch-line couplers with predetermined compact size and bandwidth. *IEEE Trans. Microw. Theory Tech.* **55**, 1926–1934 (2007)
64. Jung, S.-C., Negra, R., Ghannouchi, F.M.: A design methodology for miniaturized 3-dB branch-line hybrid couplers using distributed capacitors printed in the inner area. *IEEE Trans. Microw. Theory Tech.* **56**, 2950–2953 (2008)
65. Ahn, H.-R.: Modified asymmetric impedance transformers (MCCTs and MCVTs) and their application to impedance-transforming three-port 3-dB power dividers. *IEEE Trans. Microw. Theory Tech.* **59**, 3312–3321 (2011)
66. Tseng, C.-H., Chang, C.-L.: A rigorous design methodology for compact planar branch-line and rat-race couplers with asymmetrical T-structures. *IEEE Trans. Microw. Theory Tech.* **60**, 2085–2092 (2012)
67. Ahn, H.-R., Nam, S.: Compact microstrip 3-dB coupled-line ring and branch-line hybrids with new symmetric equivalent circuits. *IEEE Trans. Microw. Theory Tech.* **61**, 1067–1078 (2013)
68. Eccleston, K.W., Ong, S.H.M.: Compact planar microstripline branch-line and rat-race couplers. *IEEE Trans. Microw. Theory Tech.* **51**, 2119–2125 (2003)
69. Chuang, M.-L.: Miniaturized ring coupler of arbitrary reduced size. *IEEE Microw. Wirel. Compon. Lett.* **15**, 16–18 (2005)
70. Chun, Y.-H., Hong, J.-S.: Compact wide-band branch-line hybrids. *IEEE Trans. Microw. Theory Tech.* **54**, 704–709 (2006)
71. Kuo, J.-T., Wu, J.-S., Chiou, Y.-C.: Miniaturized rat race coupler with suppression of spurious passband. *IEEE Microw. Wirel. Compon. Lett.* **17**, 46–48 (2007)
72. Mondal, P., Chakrabarty, A.: Design of miniaturised branch-line and rat-race hybrid couplers with harmonics suppression. *IET Microw. Antennas Propag.* **3**, 109–116 (2009)
73. Ahn, H.-R., Kim, B.: Small wideband coupled-line ring hybrids with no restriction on coupling power. *IEEE Trans. Microw. Theory Tech.* **57**, 1806–1817 (2009)
74. Sun, K.-O., Ho, S.-J., Yen, C.-C., van der Weide, D.: A compact branch-line coupler using discontinuous microstrip lines. *IEEE Microw. Wirel. Compon. Lett.* **15**, 501–503 (2005)
75. Lee, H.-S., Choi, K., Hwang, H.-Y.: A harmonic and size reduced ring hybrid using coupled lines. *IEEE Microw. Wirel. Compon. Lett.* **17**, 259–261 (2005)
76. Tseng, C.-H., Chen, H.-J.: Compact rat-race coupler using shunt-stub-based artificial transmission lines. *IEEE Microw. Wirel. Compon. Lett.* **18**, 734–736 (2008)
77. Wang, C.-W., Ma, T.-G., Yang, C.-F.: A new planar artificial transmission line and its applications to a miniaturized butler matrix. *IEEE Trans. Microw. Theory Tech.* **55**, 2792–2801 (2007)
78. Ahn, H.-R., Nam, S.: Wideband microstrip coupled-line ring hybrids for high power-division ratios. *IEEE Trans. Microw. Theory Tech.* **61**, 1768–1780 (2013)
79. Tsai, K.-Y., Yang, H.-S., Chen, J.-H., Chen, Y.-J.: A miniaturized 3 dB branch-line hybrid coupler with harmonics suppression. *IEEE Microw. Wirel. Compon. Lett.* **21**, 537–539 (2011)
80. Collin, R.E.: *Foundations for Microwave Engineering*. Wiley, New York (2001)
81. Gu, J., Sun, X.: Miniaturization and harmonic suppression rat-race coupler using C-SCMRC resonators with distributive equivalent circuit. *IEEE Microw. Wirel. Compon. Lett.* **15**, 880–882 (2005)

82. Kurgan, P., Filipcewicz, J., Kitlinski, M.: Development of a compact microstrip resonant cell aimed at efficient microwave component size reduction. *IET Microw. Antennas Propag.* **6**, 1291–1298 (2012)
83. Kurgan, P., Kitlinski, M.: Doubly miniaturized rat-race hybrid coupler. *Microw. Opt. Technol. Lett.* **53**, 1242–1244 (2011)
84. Bekasiewicz, A., Koziel, S., Zieniutycz, W.: Design space reduction for expedited multi-objective design optimization of antennas in highly-dimensional spaces. In: Koziel, S., Leifsson, L., Yang, X.S. (eds.) *Solving Computationally Expensive Engineering Problems: Methods and Applications*, pp. 113–147. Springer, Switzerland (2014)
85. Koziel, S., Ogurtsov, S.: Rapid optimization of omnidirectional antennas using adaptively adjusted design specifications and kriging surrogates. *IET Microw. Antennas Propag.* **7**, 1194–1200 (2013)
86. Hong, J.-S., Lancaster, M.J.: *Microstrip filters for RF/microwave applications*. Wiley, New York (2001)
87. Koziel, S., Bekasiewicz, A.: Simulation-driven design of planar filters using response surface approximations and space mapping. In: *European Microwave Conference* (2014)
88. Lai, M.-I., Jeng, S.-K.: A microstrip three-port and four-channel multiplexer for WLAN and UWB coexistence. *IEEE Trans. Microw. Theory Tech.* **53**, 3244–3250 (2005)
89. Balanis, C.A.: *Antenna Theory: Analysis and Design*, 2nd edn. Wiley, New York (1997)
90. Milligan, T.A.: *Modern Antenna Design*, 2nd edn. Wiley, New York (2005)
91. Koziel, S., Ogurtsov, S.: Computational-budget-driven automated microwave design optimization using variable-fidelity electromagnetic simulations. *Int. J. RF Microw. Comput. Aided Eng.* **23**, 349–356 (2013)
92. Koziel, S., Cheng, Q.S., Bandler, J.W.: Space mapping. *IEEE Microw. Mag.* **9**, 105–122 (2008)
93. Conn, A.R., Gould, N.I.M., Toint, P.L.: *Trust Region Methods*. MPS-SIAM Series on Optimization (2000)
94. Koziel, S., Kurgan, P.: Rapid design of miniaturized branch-line couplers through concurrent cell optimization and surrogate-assisted fine-tuning. *IET Microw. Antennas Propag.* **9**, 957–963 (2015)
95. Mongia, R., Bahl, I., Bhartia, P.: *RF and Microwave Coupler-line Circuits*. Artech House, Norwood (1999)
96. Sonnet: version 14.54. Sonnet Software, North Syracuse, NY, Unites States (2013)
97. Rautio, J.C., Rautio, B.J., Arvas, S., Horn, A.F., Reynolds, J.W.: The effect of dielectric anisotropy and metal surface roughness. In: *Proceedings Asia-Pacific Microwave Conference* (2010)
98. Koziel, S., Bekasiewicz, A., Kurgan, P.: Rapid EM-driven design of compact RF circuits by means of nested space mapping. *IEEE Microw. Wirel. Compon. Lett.* **24**, 364–366 (2014)
99. Agilent, A.D.S.: Version 2011 Agilent Technologies, 1400 Fountaingrove Parkway, Santa Rosa, CA 95403-1799 (2011)
100. Bandler, J.W., Cheng, Q.S., Nikolova, N.K., Ismail, M.A.: Implicit space mapping optimization exploiting preassigned parameters. *IEEE Trans. Microw. Theory Tech.* **52**, 378–385 (2004)
101. Liang, J., Chiau, C.C., Chen, X., Parini, C.G.: Printed circular disc monopole antenna for ultra-wideband applications. *Electron. Letters.* **40**, 1246–1247 (2004)
102. Li, T., Zhai, H., Li, G., Li, L., Liang, C.: Compact UWB band-notched antenna design using interdigital capacitance loading loop resonator. *IEEE Antennas Wirel. Propag. Lett.* **11**, 724–727 (2012)
103. Li, L., Cheung, S.W., Yuk, T.I.: Compact MIMO antenna for portable devices in UWB applications. *IEEE Trans. Antennas Propag.* **61**, 4257–4264 (2013)